Full title: Isoflurane and Ketamine Differentially Influence Spontaneous and Evoked Laminar Electrophysiology in Mouse V1

Abbreviated title: Laminar Electrophysiological Analysis of Isoflurane and Ketamine Anesthesia

Nicholas J. Michelson[1], Takashi D.Y. Kozai[1-5]

[1]*Department of Bioengineering, University of Pittsburgh, Pittsburgh, Pennsylvania;* [2]*Center for the Neural Basis of Cognition, University of Pittsburgh, Pittsburgh, Pennsylvania;* [3]*Center for Neuroscience, University of Pittsburgh, Pittsburgh, Pennsylvania;* [4]*McGowan Institute of Regenerative Medicine, University of Pittsburgh, Pittsburgh, Pennsylvania;* [5]*NeuroTech Center, University of Pittsburgh Brain Institute, Pittsburgh, Pennsylvania*

Corresponding Author: T. Kozai, 300 Technology Dr. 208 Center for Bioengineering, Pittsburgh PA, 15217 (email: tdk18@pitt.edu)

Abstract

General anesthesia is ubiquitous in research and medicine, yet although the molecular mechanisms of anesthetics are well characterized, their ultimate influence on cortical electrophysiology remains unclear. Moreover, the influence that different anesthetics have on sensory cortices at neuronal and ensemble scales is mostly unknown, and represents an important gap in knowledge that has widespread relevance for neural sciences. To address this knowledge gap, this work explored the effects of isoflurane and ketamine/xylazine, two widely used anesthetic paradigms, on electrophysiological behavior in mouse primary visual cortex. First, multiunit activity and local field potentials were examined to understand how each anesthetic influences spontaneous activity. Then, the inter-laminar relationships between populations of neurons at different cortical depths were studied to assess whether anesthetics influenced resting-state functional connectivity. Lastly, the spatiotemporal dynamics of visually evoked multiunit and local field potentials were examined to determine how each anesthetic alters communication of visual information. We found that isoflurane enhanced the

rhythmicity of spontaneous ensemble activity at 10-40 Hz, which coincided with large increases in coherence between layer IV with superficial and deep layers. Ketamine preferentially increased local field potential power from 2-4 Hz, and the largest increases in coherence were observed between superficial and deep layers. Visually evoked responses across layers were diminished under isoflurane, and enhanced under ketamine anesthesia. These findings demonstrate that isoflurane and ketamine anesthesia differentially impact sensory processing in V1.

NEW & NOTEWORTHY We directly compared electrophysiological responses in awake and anesthetized (isoflurane or ketamine) mice. We also propose a method for quantifying and visualizing highly variable, evoked multiunit activity. Lastly, we observed distinct oscillatory responses to stimulus onset and offset in awake and isoflurane anesthetized mice.

Keywords: anesthesia, laminar electrophysiology, spontaneous, evoked

INTRODUCTION

In 1846, the first successful surgery under general anesthesia was performed, thereafter revolutionizing the practice of medicine (Robinson and Toledo 2012). Yet after more than a century of clinical ubiquity, a detailed understanding of the micro and mesoscale mechanisms of anesthesia and anesthetic induced loss of consciousness remains elusive. Consciousness is thought to emerge from the integration of information generated from subsystems across the brain (Tononi 2008). Accordingly, anesthetic induced unconsciousness is characterized by disruption of communication between cortical or subcortical networks (Alkire et al. 2008; Franks 2008; Hudetz 2012; Mashour and Hudetz 2018). To this end, many studies have investigated how various anesthetics influence or restrict large-scale functional communication between brain regions (Boveroux et al. 2010; Cimenser et al. 2011; Schroeder et al. 2016; Sellers et al. 2015; Supp et al. 2011).

Fewer studies, however, explore the effects of anesthesia at the local ensemble scales. Yet growing evidence suggests that anesthetics have a profound influence on neuronal network activity

within cortical subsystems. For example, anesthetics have been shown to alter the balance between excitation and inhibition (Haider et al. 2013; Homayoun and Moghaddam 2007), modulate oscillatory ensemble activity (Chery et al. 2014; Hakami et al. 2009; Imas et al. 2004; Imas et al. 2005), and influence neuronal response properties (Duncan et al. 1982; Goltstein et al. 2015). These changes in neuronal activity are important to characterize since many seminal neuroscience studies have been conducted in anesthetized animals, and a detailed understanding of the electrophysiological effects of anesthetics may be critical for an accurate interpretation of results.

Moreover, numerous anesthetic agents, which have distinct molecular targets, electrophysiological features, and act with regional specificity, have been widely used throughout the literature (Brown et al. 2011; Cavazzuti et al. 1987). Direct comparisons of anesthetic classes have revealed substantial variability in altered electrophysiological behavior (Cederholm et al. 2012; Furmaga et al. 2014; Hayton et al. 1999; Ruebhausen et al. 2012; Sarasso et al. 2015; Woodward et al. 2007). A detailed comparison of micro and mesoscale cortical activity between anesthetic classes may therefore provide further insight into the mechanistic actions of anesthetics. The present work compares network activity using a linear electrode array, under isoflurane and ketamine/xylazine (KX) anesthesia, two commonly used anesthetic paradigms in neuroscience research.

Isoflurane is a volatile anesthetic, which acts primarily via potentiation of inhibitory $GABA_A$ (gamma-aminobutyric acid type A) receptors, but also through inhibition of glutamatergic AMPA (α-amino-3-hydroxy-5-methyl-4-isoxazolepropionic acid) and NMDA (N-methyl-D-aspartate) receptors (Alkire et al. 2008; Dildy-Mayfield et al. 1996; Kimbro et al. 2000). Isoflurane administration affects cortical activity in a dose-dependent fashion, progressing towards burst suppression at high concentrations, which is characterized by quasi-periodic alternations of high amplitude bursting activity followed by prolonged periods of suppressed activity (Ferron et al. 2009). In sensory cortices, isoflurane augments spontaneous and evoked local field potential (LFP) oscillations (Imas et al. 2005; Sellers et al.

2013; Sellers et al. 2015), and alters the spatial and temporal dynamics of evoked multiunit activity (MUA), possibly as a result of diminished inhibition (Haider et al. 2013).

Ketamine, a dissociative anesthetic, acts primarily via inhibition of NMDA receptors, but also through minor potentiation of $GABA_A$ receptors (Alkire et al. 2008; Brown et al. 2011). It is often used with the sedative xylazine, an α_2 adrenergic receptor agonist. In cortex, ketamine produces disinhibited excitation, and strongly influences oscillatory LFP, particularly by inducing prominent slow wave activity (Chauvette et al. 2011; Fiáth et al. 2016; Steriade et al. 1993b) and modulating gamma frequencies (Anver et al. 2011; Caixeta et al. 2013; Chery et al. 2014; Hakami et al. 2009; Shaw et al. 2015). Interestingly, ketamine shares similar electrophysiological abnormalities with schizophrenia (Caixeta et al. 2013; Ehrlichman et al. 2009).

Although isoflurane and ketamine have been extensively studied independently, this study aims to build upon this body of knowledge by directly comparing laminar electrophysiological activity within the same animals. Recordings were collected from mouse V1 because the functional architecture of the visual system is well documented; information flows from layer IV to II/III, then V (Douglas and Martin 2004; Hirsch and Martinez 2006). Additionally, recordings from the visual cortex provide the capability to examine spontaneous and evoked activity. To this end, we examined multiunit activity and local field potentials to provide insight into the functional changes in individual neurons, as well as the summated population activity within the surrounding area. Isoflurane and ketamine were found to produce spatiotemporally and rhythmically distinct patterns of spontaneous and evoked electrophysiological activity, suggesting that processing within V1 is differentially influenced by each anesthetic.

METHODS

All experimental protocols were approved by the University of Pittsburgh's Institutional Animal Care and Use Committee.

Surgical Procedure

Surgical procedures were carried out as previously described (Kozai et al. 2015a; Kozai et al. 2015b; Kozai et al. 2014; Michelson et al. 2017). 9-week old female C57BL/6 mice (22-28g) were placed in a stereotaxic frame (Kopf Instruments, Tujunga, CA) and induced with 1.5–2% isoflurane with oxygen flow at 1 L/min, and then maintained at 1.25–1.5%. Throughout the procedure, body temperature was maintained using a warm water pad (HTP 1500, Adroit Medical Systems, Loudon TN). After the skin and connective tissue over the skull were removed, a thin layer of Vetbond (3 M) was applied to the skull. A small craniotomy was made over visual cortex with a high-speed dental drill. The drilling procedure was periodically interrupted, and the surface of the skull rinsed with a saline solution to prevent damaging heat transfer to the brain. Three bone screws were placed into the skull, one over the contralateral visual cortex and two bilaterally over motor cortex.

A 16-channel, planar silicon Michigan electrode (single shank, 3mm long, recording sites spaced 100µm apart; A1 × 16-3mm-100-703-CM16LP, Neuronexus Technologies, Ann Arbor, MI) was implanted into the left monocular visual cortex (1.0mm anterior to lambda, 1.5mm lateral from midline). The array was inserted at ~1mm/s to a depth of 1.6mm, using a hand-driven micromanipulator, such that the top edge of the top-most recording site was at the surface of the brain, and the recording sites faced away from the midline, toward V1m/V1b. The reference wire was connected to the ipsilateral bone screw over the motor cortex, and the preamplifier ground wire was shorted to the contralateral bone screws over the motor and visual cortex. After insertion, the craniotomy was filled, and the electrode was protected with Kwik-sil. The electrode and bone screws were then cemented into place with dental cement (Pentron Clinical, Orange, CA). After the procedure, 3cc of Ringer's solution was injected subcutaneously to the back of the animal to aid recovery. Buprenorphine (0.3 mg/kg) was administered twice daily for three days as a post-operative analgesic.

Neurophysiological Recording

Chronic electrophysiological recordings (183-190 days post-implant) were conducted from within a grounded, but otherwise electrically isolated faraday cage. Each animal was recorded for a single time-point. A 24" LCD screen (V243H, Acer. Xizhi, New Taipei City, Taiwan) was placed just outside of the cage for presentation of visual stimulus. Recorded data was transferred through a nonconductive optic fiber out of the cage, using a battery-powered preamplifier (Medusa preamp, Tucker-Davis Technologies, Alachua, FL), which was housed inside the cage (Kozai et al. 2012).

Animals were placed on a microwaveable heating pad (Deltaphase isothermal pad, Braintree Scientific, Inc, Braintree, MA) (1.6 mm mesh), with the head mechanically fixed using a custom-built stereotaxic frame. The animal was placed 20cm from the monitor on the side contralateral to the site of implantation, spanning a total visual field of 120° wide by 60° high. Recordings were conducted in a dark room and consisted of 130s epochs of spontaneous and visually evoked signals, sampled at 24kHz. Spontaneous recordings were taken with the monitor turned off. For the evoked recordings, visual stimuli were presented using the MATLAB-based Psychophysics Toolbox (Psychtoolbox) (Brainard 1997; Kleiner et al. 2007; Pelli 1997). Stimuli consisted of full-field solid black and white drifting gratings in vertical or 45° directions. Timing of the visual stimulus was synchronized to the recording system (RX5, Tucker-Davis Technologies, Alachua FL) via transistor-transistor logic (TTL) pulses sent from the display computer through a stimulus isolator (A-M Systems Model 2200). 64 visually evoked trials were conducted throughout the recording epoch, where each trial consisted of 1 second of stimulus presentation followed by a 1 second dark screen period (Cody et al. 2018; Kolarcik et al. 2015; Kozai et al. 2016; Kozai et al. 2015b), hereafter referred to as ON and OFF periods.

Six animals were examined in this study. Data were first collected from lightly isoflurane-anesthetized animals. Recordings began 10 minutes following isoflurane induction. Dosage was maintained at the lowest concentration sufficient for inducing animal inactivity while avoiding burst suppression (Kozai et al. 2015b) (~1.1%). Animals were carefully monitored during recording to ensure

that this level of anesthesia was maintained. Following data collection, isoflurane administration ceased, and animals recovered for at least 30 minutes before awake trials began. After awake data collection, animals were deeply anesthetized with an intraperitoneal injection of 90 mg/kg ketamine and 9mg/kg xylazine cocktail. Data collection began approximately 10 minutes following injection.

Electrophysiological Signal Processing

The raw data was filtered using a 2nd order Butterworth filter to produce LFP (passband 2–300 Hz) and spike streams (passband 300–5000 Hz). Common average referencing was applied to the filtered data (Ludwig et al. 2009). Multi units were identified by establishing a threshold for the high-frequency data at 3.5 standard deviations below the mean, as previously published (Kozai et al. 2012). The noise floor of the spike-stream was calculated as 2σ, where σ is the standard deviation of the spike-stream over the entire recording duration after removing all threshold crossing events.

Data Analysis

All data analysis was performed in MATLAB. Comparisons between evoked and spontaneous activity, or between brain states, were conducted on the same electrode site from the same animal. Boxplots were used to show the distribution of the data. In each boxplot, the median is represented by the horizontal line, the interquartile range is shown by the edges of the box, and the whiskers extend from the 5th to the 95th percentile. Outliers are denoted by circles and the sample mean is shown with a black X. In order to compare spontaneous and evoked activity, 64 uniformly spaced pseudo-triggers were inserted throughout the spontaneous recording epoch, similar to the spacing of visual stimuli. Evoked activity (i.e. activity following stimulus presentations) was then compared to activity following pseudo-triggers. All spectral analyses were computed using the Chronux toolbox (Bokil et al. 2010; Mitra 2007) in MATLAB.

Analysis of Multi Unit Activity

The number of multiunit threshold crossing events that occurred within a 1-second period following each stimulus presentation or pseudo-trigger was recorded. Peri-stimulus time histograms with 50ms bins were generated to show the dynamics of the multiunit response. Average multiunit firing rates were calculated using the average number of threshold crossing events within a 1-second period following each pseudo-trigger.

Multiunit yield is a recording performance metric that describes the functional reactivity of the surrounding tissue. Yield was defined as the percentage of electrode sites which recorded a significantly different ($p < 0.05$) multiunit spike count during visual stimulation (ON condition, after stimulus onset) compared to background activity (OFF condition, before stimulus onset). To quantify evoked responses, the multiunit yield and signal to noise firing rate ratio (SNFRR) were calculated (Kozai et al. 2015b). The SNFRR (Eq. 1) compared the difference in MUA between stimulus conditions relative to the average standard deviation of each stimulus conditions:

(1) $$SNFRR = \frac{\mu_{ON} - \mu_{OFF}}{\frac{1}{2}(\sigma_{ON} + \sigma_{OFF})}$$

where μ_{ON} and μ_{OFF} are the mean firing rates across trials during the ON and OFF conditions, and σ_{ON} and σ_{OFF} are the standard deviations of the firing rates during the ON and OFF conditions. Yield and SNFRR were parameterized by the duration of the temporal bins within the ON and OFF conditions that are being compared and the latency of each bin following stimulus onset.

Analysis of Local Field Potentials

Negative deflections in the LFP have been shown to be correlated with neuronal firing rate and synchrony (Petermann et al. 2009). Therefore, the magnitude of synchronous LFP voltage activity was quantified using the peak-to-peak amplitude, to capture potentially relevant after-hyperpolarizations (Buzsaki et al. 2012; Kozai et al. 2015b). The sum of the full-wave rectified LFP (Kozai et al. 2015b) was also calculated as a measure of the degree to which the LFP voltage activity is temporally sustained. Calculations were performed over a 1s period following each pseudo-trigger or stimulus presentation.

To examine the visual stimulus' contribution to the evoked LFP response, the LFP was normalized by subtracting the spontaneous activity (amplitude or sum) from the evoked.

Spectral power of the LFP was calculated with the multi-taper method using a duration of 1s, a half-bandwidth of 1Hz and a taper number of 1. Relative power was measured as the ratio of the power within a specified frequency band to the broadband power (Eq. 2). Evoked power spectral densities were normalized by subtracting the log transformed spontaneous power spectrum from the log transformed evoked power spectrum (Eq. 3).

(2) $R = \frac{\sum_a^b S(f)}{\sum S(f)}$

(3) $N(f) = 10\log_{10}[\frac{S_E(f)}{S_{RS}(f)}]$

where *R* is relative power, *S(f)* is the power spectrum of the LFP, *a* and *b* are the lower and upper frequencies of the specified frequency range, *N(f)* is the normalized power spectrum, and $S_E(f)$ and $S_{RS}(f)$ are the evoked and resting state power spectra respectively.

The laminar relationship between LFPs at different depths was quantified using the magnitude-squared coherence, which describes the similarity between two signals as a function of frequency. Coherence values range from 0 to 1, indicating either no relationship or a perfect linear relationship between signals, respectively. The coherence is given by equation 4:

(4) $C_{xy}(f) = \frac{S_{xy}(f)}{\sqrt{S_{xx}(f)S_{yy}(f)}}$

(5) $\Delta C_{xy}(f) = C_{xy}^{E}(f) - C_{xy}^{RS}(f)$

where $C_{xy}(f)$ is the coherence, $S_{xy}(f)$ is the cross-spectrum, $S_{xx}(f)$ and $S_{yy}(f)$ are the auto-spectra of the LFP from electrode sites *x* and *y* respectively. Coherence was calculated on the 1-second interval following each stimulus or pseudo-trigger, using a half-bandwidth of 3Hz and a taper number of 5, and then averaged across trials. Normalized coherence (Eq. 5) is calculated as the difference between the evoked coherence and the resting-state coherence. To assess coherence between layers, the coherence

between all electrode sites located within each respective layer were averaged to yield an estimate of the coherence between regions. Coherence values for specified frequency bands are given by the mean coherence within that frequency band. This estimate was then averaged across animals to compare coherence across anesthetics.

Assignment of cortical layers

Current source density (CSD) analysis was performed by computing the second derivative of the stimulus-locked LFP voltage trace with respect to depth, and then averaged across trials. To account for a degree of uncertainty in layer assignment, putative layer IV was defined to include the two electrode sites which encompassed the location of the first evoked current sink. This first evoked current sink was defined as the minimum value of the CSD that occurred within the first 100ms following visual stimulus presentation. Given the electrode site spacing of 100µm, this definition describes a 'viewing distance' of approximately 300µm. This method has previously been verified with post-mortem histology (Kozai et al. 2014). All laminar analyses between animals were first aligned to layer IV.

Statistical Analysis

For each comparison, normality was first assessed using the Kolmogorov-Smirnov test. If all groups were normally distributed, differences between groups were calculated using a repeated measures one-way analysis of variance (ANOVA). When one or more groups did not follow a normal distribution, a Friedman's ANOVA was performed. Post-hoc significance was confirmed using paired t-tests for normally distributed data, or Wilcoxon signed-rank tests for non-normally distributed data. Post-hoc confidence was accounted for using a Bonferroni correction.

RESULTS

Spontaneous Multiunit and LFP

Resting-state activity was first examined to understand how each anesthetic influences spontaneous cortical processing. Periodic bursts of multiunit activity were observed under KX anesthesia

(Fig. 1a), matching large deflections in the LFP (Fig. 1b). Average firing rates over one second trial durations were greater under KX compared to awake (Fig. 1c, p=0.01; n=96 electrode sites, Friedman's ANOVA), but no significant differences in firing rate were observed between anesthetics, or between isoflurane and awake. LFP peak-to-peak amplitude was significantly greater under anesthesia compared to awake ($p<0.001$, n=96 electrode sites, Friedman's ANOVA), and under KX compared to isoflurane ($p=0.001$). LFP sum was also significantly greater under anesthesia, and under KX compared to isoflurane (Fig. 1e, $p<0.001$, n=96 electrode sites). It is possible that the increased LFP activity under isoflurane, in the absence of increased firing rates or bursting, may be caused by increased firing in cells located further than can be adequately resolved with multiunit recordings (Henze et al. 2000). Since the amplitude of extracellularly recorded action potentials is proportional to $1/r^2 - 1/r$, where r is distance from the neuronal point source (Mechler and Victor 2012; Wellman et al. 2017), a consistent increase in multiunit activity from neurons located just outside the detection range would result in recorded amplitudes just below the spike detection threshold, elevating the noise floor. Thus, to determine whether increased population activity under isoflurane anesthesia was responsible for the increases in LFP activity, despite the lack of increase in local firing rates, the noise of the spike streams was compared. Significant differences in the noise floors were not observed between brain states (Fig. 1f). The results demonstrate that KX produces synchronous bursts of multiunit activity, and both anesthetics influence the rhythmicity of ensemble activity.

Spontaneous oscillatory population activity

To explore this further, the spectral content of the LFP was examined. Anesthetics generally produced an increase in LFP power (Fig. 2a-d, $p<0.001$; n=96 electrode sites, Friedman's ANOVA), but the greatest increases occurred at distinct frequencies. Isoflurane selectively increased power at alpha and beta frequencies (8-30 Hz), while KX markedly increased power at delta frequencies (2-4 Hz)(Fig. 2b,e-f). Similar patterns of frequency-selective enhancement of power were observed across the depth

of the cortex (Fig. 2f-g). Note that although power at gamma frequencies was increased under KX anesthesia (Fig. 2b,f), the relative gamma band power was diminished (Fig 2g). These findings show that isoflurane and ketamine augment rhythmic activity at distinct frequencies.

Spontaneous laminar coherence

Oscillatory activity is hypothesized to play an active role in facilitation of communication. Therefore, laminar LFP coherence was measured to examine the relationship between population activity at different cortical depths (Maier et al. 2010). In the awake state, coherence between supragranular (SG) and infragranular (IG) layers was slightly elevated (Fig. 3a) compared to inter-laminar coherence between different regions (e.g. granular-supragranular (G-SG) or granular-infragranular (G-IG)). However, under isoflurane anesthesia, G-IG and G-SG coherence was typically greater than SG-IG coherence (Fig. 3a-b). Averaged coherence between 7-90 Hz was significantly greater in isoflurane anesthetized mice than in awake conditions, for each pair of regions (SG-IG, $p=0.005$; G-IG, $p=0.013$; G-SG, $p=0.013$; $n=6$ mice, one-way ANOVA). Ketamine increased coherence slightly between all layers, but this increase was most pronounced between SG-IG regions ($p=0.05$). These findings demonstrate that anesthetics influence the functional relationship between LFP activity across layers.

Quantification of evoked multiunit activity

Having established that isoflurane and ketamine differentially influence resting-state network activity, we next asked whether evoked cortical responses differed between anesthetics. As expected, visually evoked responses demonstrate considerable temporal differences across anesthetics (Fig. 4a-b). The MU yield and signal to noise firing rate ratio (SNFRR) were compared between visual stimulation to the pre-stimulus intervals, to evaluate the responsiveness of the tissue under each anesthetic. Yield and SNFRR were calculated by comparing multiunit activity within bins, before and after the stimulus, and are therefore dependent on parameters such as bin duration and latency from stimulus onset. However, as the evoked responses demonstrated considerable temporal differences, the parameters for

measuring yield and SNFRR will similarly differ. To address this, the yield and SNFRR were calculated for multiple combinations of temporal bin sizes and latencies for each channel (Fig. 4b). Bin size was varied from 0.5 to 1000ms, with a temporal resolution of 0.5ms; and latency from stimulus onset was varied from 0 to 999.5ms, with a resolution of 0.5ms. MU yield and SNFRR were calculated for all combinations of bin sizes (*B*) and latencies (*L*) that remained within the 1s ON period, such that $B + L \leq 1s$. Previous studies have demonstrated that incorporating a negative latency may improve yield with periodic stimulation due to the OFF response (Kozai et al. 2015b). To explore this observation, yield and SNFRR were also calculated for all possible combinations of negative latencies ranging from 0 to 100ms, with positive latencies ranging from 0 to 200ms; and bin widths ranging from 0 to 1000ms; each with a temporal resolution of 1ms.

MU yield and SNFRR as a function of bin size and latency were visualized to characterize temporal differences between multiunit responses (Fig. 4c-e). Yield and SNFRR showed consistent and distinct patterns of MU dynamics between brain states. Awake animals had strong, transient responses, which were followed by a weaker, sustained response (Fig. 4c), reflecting classical visually evoked firing rate responses. In contrast, isoflurane anesthesia abolished the transient response and produced a weak, sustained response (Fig. 4d). Evoked MUA under KX demonstrates the existence of a strong transient response, and a consistent pre-stimulus burst and/or post-transient lull in MUA, followed by a rebounding increase in MUA towards the end of the stimulus period (Fig. 4e). The optimal parameters for quantifying evoked yield in each condition demonstrate that the transient response is more prolonged under KX anesthesia than awake (Fig. 4f-g). These findings suggest that isoflurane and ketamine alter the temporal dynamics of evoked multiunit responses.

Laminar multiunit and LFP response to visual stimulus

The precise number and timing of multiunit events has important implications for the representation and transmission of information. Therefore, laminar responses to the visual stimuli were

examined, to further explore how each anesthetic may alter the processing of visual signals. Averaged firing rates against cortical depth and time, show laminar patterns of activity that are consistent with those suggested by the previous analysis (Fig. 5a). Namely, strong transient responses are observed in awake and KX anesthetized mice, while weak, sustained responses occur under isoflurane. This weak, sustained response is limited to input layers. Additionally, periodic bursts of MUA under KX became entrained to visual stimuli, and transient responses can be observed after the start of OFF periods. Current source density analysis averaged across 64 stimuli and then across animals, shows prominent sinks across layers in awake and KX anesthetized animals, and diminished sinks across layers in isoflurane anesthetized animals (Fig. 5b). Additionally, KX anesthetized mice have a more prolonged CSD response. Evoked LFP peak-to-peak amplitude and sum in the awake mice exceeded the isoflurane response (Fig. 5c-d, $p<0.001$; n=96 electrode sites, Friedman's ANOVA), and were comparable to the ketamine response after normalization (Fig. 5e-f, $p=0.02$). These findings demonstrate that visual processing within and between layers are differentially altered by each anesthetic agent.

Laminar coherence during visual stimulus presentation

Since spatiotemporally distinct responses were demonstrated in multiunit and LFPs between isoflurane and ketamine, laminar coherence was examined to further assess the extent to which each anesthetic impaired or altered functional communication through V1. Upon visual stimulus presentation, coherence within superficial layers became elevated in awake animals (Fig. 6a). However, isoflurane did not produce large changes in coherence across depth after visual stimulus presentation. Under KX anesthesia, coherence between G-IG and G-SG layers, as well as within superficial and deep layers became elevated (Fig 6a-c). Both anesthetics had significantly greater evoked inter-laminar LFP coherence (Iso: SG-IG and G-IG $p=0.002$; G-SG, $p=0.003$; KX: SG-IG, $p=0.004$; G-IG and G-SG, $p=0.04$; n=6 mice, one-way ANOVA). These findings demonstrate that both anesthetics influence the relationship between evoked population activity across layers.

Differential responses to stimulus ON and OFF periods

As a strong transient response was observed under KX during OFF periods, the evoked power in response to stimulus OFF were examined for each anesthetic, and compared to the ON response. To dissociate the effect of visual stimulation from the effects of anesthesia, evoked power was normalized by subtracting the spontaneous power spectrum from the same electrode site (Fig. 7a-d). In response to stimulus ON, the power in awake and isoflurane anesthetized mice remains relatively unchanged, with the exception of a gamma peak. This ON response peak was more prominent, and occurred approximately 10Hz slower under isoflurane (Fig. 7a,b,e). Stimulus OFF in awake animals induced a slight increase in power across cortical depth that occurred at approximately 20 Hz slower than the ON response (Fig. 7f). Similarly, in isoflurane anesthetized mice, the OFF response was more pronounced compared to awake, and occurred at approximately 20 Hz slower than the ON response (Fig. 7c,d,f). In contrast, both ON and OFF periods exhibited increased power at delta and gamma-high gamma frequencies under KX anesthesia, with no obvious ON or OFF peaks (Fig. 7e). Interestingly, although the ON and OFF periods showed distinct multiunit and oscillatory responses across anesthetics, normalized coherence across layers exhibited a similar pattern during ON and OFF periods (Fig. 8a-c). Coherence during the OFF period was greater under anesthesia (Iso: SG-IG and G-IG: $p=0.002$; G-SG $p=0.001$; KX: SG-IG $p=0.004$; G-IG $p=0.03$; G-SG $p=0.02$; $n=6$ mice, one-way ANOVA). These findings imply that the processing of visual stimuli is differentially altered between anesthetics, as ON and OFF stimuli elicit distinct oscillatory responses in awake and isoflurane anesthetized animals, while KX anesthetized mice fail to exhibit this differentiation, despite having a pronounced transient multiunit response.

DISCUSSION

This study explored the impact of anesthetic agents, isoflurane and ketamine, on spontaneous and evoked electrophysiological activity in mouse primary visual cortex. The effects of each anesthetic agent on multiunit and LFP activity were examined using intracortical electrodes. Then, coherence

between populations of neurons residing at different depths was measured to gain insight into the structure of communication across layers, and how this may be influenced by anesthesia. Results indicate that although isoflurane and ketamine have overlapping molecular targets, they produce distinct electrophysiological changes, which likely reflect differentially impaired signal transduction through the cortex.

Distinct oscillatory patterns of spontaneous activity under isoflurane and ketamine anesthesia

Sleep and anesthesia induce rhythmic behavior, characterized by spindle (alpha, ~7-14 Hz), delta (~1-4 Hz), and slow wave activity (~0.3 Hz) (Steriade et al. 1993a; Steriade et al. 1993b), with the emergence of slower rhythms generally indicating progression into deeper states of sleep. KX anesthetized mice exhibited pronounced delta rhythms, as well as slow, periodic bursts of multiunit activity that were likely coupled to up states during slow oscillations (Chauvette et al. 2011; Fiáth et al. 2016). Isoflurane also increased delta power, but relative delta power was significantly lower than under ketamine anesthesia. Additionally, no qualitative evidence could be found for bursting multiunit activity at slow rhythms under isoflurane anesthesia. Since care was taken to avoid inducing burst suppression in the isoflurane anesthetized mice, these findings indicate that isoflurane induced animals likely had not reached the same depth of anesthesia as was achieved with ketamine/xylazine. However, this level of anesthesia was necessary in order to evoke cortical activity under isoflurane anesthesia. This difference in anesthetic depth represents an important consideration when interpreting the data.

In addition to the induction of delta oscillations, ketamine is known to increase and modulate power at high frequencies (Anver et al. 2011; Hakami et al. 2009; Shaw et al. 2015). Power across the gamma range and at higher frequencies showed broad increases under ketamine anesthesia. These abnormalities may stem from ketamine's primary action as an NMDA receptor antagonist. NMDAR antagonists preferentially inhibit GABAergic interneurons, causing disinhibition, or aberrant excitation

(Brown et al. 2011; Homayoun and Moghaddam 2007). Accordingly, spontaneous firing rates increased under ketamine anesthesia.

Although isoflurane also inhibits NMDA receptors and decreases cortical inhibition (Haider et al. 2013), no significant differences in spontaneous firing rates could be identified under isoflurane anesthesia compared to awake animals. This may be due to isoflurane's potentiation of $GABA_A$ receptors and inhibition of AMPA receptors (Alkire et al. 2008). $GABA_A$ receptors are prevalent throughout the cortex and their potentiation results in widespread hyperpolarization of pyramidal neurons (Bai et al. 1999; Brown et al. 2011; Garcia et al. 2010; Sigel and Steinmann 2012). AMPA receptors are glutamatergic post-synaptic receptors, which, in the visual cortex, facilitate excitatory feedforward activity (Self et al. 2012; van Kerkoerle et al. 2014).

Despite the lack of an increase in firing rate, resting-state LFP activity and broadband power increased under isoflurane anesthesia, demonstrating that isoflurane increases the rhythmicity of ensemble activity. A previous examination of resting-state activity in ferret V1 under isoflurane/xylazine anesthesia, found that anesthesia did not increase broadband power in visual cortex (Sellers et al. 2013). The reason for this discrepancy is unclear, but may be related to the use of xylazine. α2-adrenergic agonists, such as xylazine, decreased firing rates of spontaneous and visually driven cells in rat visual cortex (Kolta et al. 1987), and decreased gamma band power in the olfactory bulb (Chery et al. 2014). Interestingly, relative power under isoflurane anesthesia was greatest, compared to the other two groups, within alpha and beta frequency bands (7-30 Hz).

Functional implications for oscillatory dynamics

Neuronal oscillations may play an important role in mediating communication between neurons and cortical regions. In this regard, slow rhythms are typically thought to obstruct communication. For example, large amplitude, hypersynchronous slow waves during sleep and anesthesia are thought to disrupt the processing and communication of information, and thus be related to loss of consciousness

(Franks 2008). Similarly, frontal alpha hypersynchrony disrupts communication between brain regions and occurs concomitantly with loss of consciousness (Cimenser et al. 2011; Supp et al. 2011). In visual cortex, alpha rhythms may be associated with active suppression of information processing (Klimesch et al. 2007; Worden et al. 2000) and gamma rhythms with feature encoding and attention (Fries et al. 2001; Singer and Gray 1995). However, the functional role of gamma rhythm is subject to debate (Cardin 2016; Fries 2009; Jia et al. 2011; Ray and Maunsell 2010; 2015). Nevertheless, gamma oscillations reflect intrinsic properties of network activity, and are associated with $GABA_A$ receptor mediated inhibition, and fast-spiking parvalbumin-expressing (FS PV) inhibitory interneurons (Buzsáki and Wang 2012; Carlen et al. 2012). Evoked responses to stimulus ON and OFF periods elicited pronounced gamma oscillations under isoflurane anesthesia, which occurred at lower frequencies, than awake. This might be due to isoflurane's potentiation of the $GABA_A$ receptor, which prolongs the deactivation time of the GABA-induced current, and may thus decrease the frequency of the evoked gamma oscillation (Bai et al. 1999; Brunel and Wang 2003; Wang and Buzsáki 1996).

Interestingly, OFF periods in both awake and isoflurane anesthetized states demonstrated a consistently slower gamma response than was evoked during ON periods. Gamma oscillation frequency in V1 has been shown to be sensitive to contrast (Ray and Maunsell 2010). However, to our knowledge, distinct and consistently induced gamma oscillations have not been observed in response to contrast-OFF stimuli. Another possible origin for this response might be the luminance decrement associated with the stimulus turning off. Light and dark stimuli are processed through separate pathways in the retina and thalamus, but within the cortex, the segregation of these signals is less clearly understood. Asymmetries in cortical neuronal response properties between light and dark stimuli have been observed (Kremkow et al. 2014), and recent work has identified small groups of neurons in layer II/III that respond strongly to either ON or OFF stimuli (Smith et al. 2015). Perhaps these distinct oscillatory responses reflect differences in excitatory/inhibitory responses to contrast or luminance decrements.

However, the physiological mechanism underlying this response is currently unclear and can be explored more systematically in future work.

Differential effects of isoflurane and ketamine on laminar communication

A pattern of highly coherent, intra-laminar spontaneous activity under isoflurane anesthesia was observed, with relatively weak SG-IG coherence, compared to G-IG or G-SG. This pattern contrasts with that of the awake or ketamine anesthetized mice, which exhibited comparable or slightly elevated SG-IG coherence (compared to G-IG or G-SG coherence) and suggests that isoflurane alters the communicative relationship between layers. Visually evoked multiunit responses were diminished and temporally sustained in layer IV under isoflurane anesthesia. Correspondingly, evoked LFP peak-to-peak amplitude was generally smaller than spontaneous, indicating that rhythmic baseline activity was disrupted by visual stimulation in such a way that decreased the synchronicity of ensemble activity. Pronounced current sinks observed in layers IV and II/III, and weaker sinks seen in layer V, further suggest that isoflurane disrupts the temporal organization of visual stimulus induced local field potentials. Following visual stimulation, laminar coherence remained significantly elevated compared to awake, and exhibited only slight changes in coherence compared to spontaneous activity.

Ketamine was also shown to increase resting-state coherence between layers. However, the pattern of coherence between and within layers under ketamine anesthesia remained similar to that of awake animals. Visually evoked multiunit yield and optimal bin sizes to measure yield, were each greater under ketamine anesthesia than awake, suggesting that the transient response was both more pronounced and sustained. Additionally, visual stimuli appear to have entrained spontaneous bursting multiunit activity, such that bursts coincide temporally with stimulus changes (OFF-ON and ON-OFF), thereby maximizing neuronal responsiveness (Hasenstaub et al. 2007; Shu et al. 2003). Robust current sinks in layers IV, II/III and V suggest effective signal propagation across the cortex. Laminar coherence increased after visual stimulation within superficial and deep layers, as well as between regions, even at

higher frequencies. As gamma coherence is spatially restricted (Jia et al. 2011), this may reflect functional communication between anatomical connections (Douglas and Martin 2004; Hirsch and Martinez 2006). Taken together, the data suggests that isoflurane anesthesia suppressed while ketamine enhanced laminar communication in V1.

Conclusion

The chronic nature of this experiment introduces the possibility for confounds, such as electrode failure (Barrese et al. 2013; Wellman et al. 2017), altered neuronal gene expression following chronic exposure to isoflurane (Kaneko et al. 2005), or changes in visual response properties due to age related changes to visual cortex physiology (Mendelson and Wells 2002; Polidori et al. 1993). However, since direct pairwise comparisons were made within animals, these experimental confounds were minimized. Additionally, 8-9 month old mice are not expected to exhibit significantly different changes in visual acuity or contrast sensitivity than younger mice (Lehmann et al. 2012).

Our results indicate that although isoflurane and ketamine share numerous molecular targets, they exhibit distinct spontaneous network behaviors and differentially alter laminar processing in visual cortex. These findings demonstrate that different anesthetics may present different circuit level electrophysiological behaviors, which may be an important consideration for studies that draw physiological conclusions from experiments on anesthetized animals. Further comparative analyses should therefore be conducted in this area to characterize dose dependent changes in laminar activity across a more exhaustive list of anesthetic regimes. For example, urethane is a widely used anesthetic agent for acute neurophysiological studies, and further analysis in this regard will provide important information for future studies. This type of analysis may ultimately allow for a more careful selection of appropriate anesthetic agents. Additionally, these differences may provide insight into how perturbed network activity contributes to altered brain states during unconsciousness or as a result of neurological disorders.

ACKNOWLEDGEMENTS

The authors would like to thank Drs. Anthony Hudetz and Matthew Smith for helpful discussions and revisions on the manuscript, and Dominic Dawes for assistance on quantifying evoked multiunit activity.

GRANTS

This work was supported financially by NIH R01NS094396, R01NS089688 and R01NS062019.

DISCLOSURES

No conflicts of interest, financial or otherwise, are declared by the authors.

AUTHOR CONTRIBUTIONS

T.D.Y.K. and N.J.M. conception and design of research; T.D.Y.K. performed experiments; N.J.M. analyzed data; N.J.M. and T.D.Y.K. interpreted results of experiments; N.J.M. prepared figures and drafted manuscript; N.J.M. and T.D.Y.K. edited and revised manuscript, and approved final version of manuscript.

Figure Captions

Figure 1: Anesthetics alter temporal aspects of resting state population activity. a) Representative spike streams recorded from layer IV in the same animal at the same electrode site. MUA under ketamine anesthesia exhibits bursting characteristics. b) LFPs corresponding to spike streams from (a). Large, negative deflections in the ketamine example match bursts in the MUA. c) Average firing rates along the length of the electrode shank, computed over one second intervals, were slightly greater under ketamine anesthesia. Amplitude of the noise floor did not differ significantly across anesthetics. d-e) LFP peak to peak amplitude and sum are significantly greater under anesthesia. Ketamine has significantly greater LFP activity than isoflurane. f) Amplitude of the noise floor did not differ significantly across anesthetics. (n=96 electrode sites: * $p<0.001$, # $p=0.001$, % $p=0.01$)

Figure 2: Isoflurane and ketamine increase resting-state power at distinct frequencies. a) Representative power spectra, recorded from layer IV in the same animal at the same electrode site. b) Power spectra from (a), normalized by subtracting the awake spectrum from the anesthetized. c-d) Anesthesia significantly increases mean and peak power, along the depth of the cortex. e) Awake induced LFP power against depth, averaged across pseudo-triggers, and then animals. Depth is relative to layer IV, indicated by the dotted black regions. f) Averaged power against depth under isoflurane and ketamine anesthesia, normalized to awake, as in (b). Largest increases in power occur at alpha and beta frequencies under isoflurane, and delta and gamma frequencies under ketamine. g) Relative power within frequency bands are differentially affected by isoflurane and ketamine. (n=96 electrode sites: * $p<0.001$, # $p=0.002$)

Figure 3: Resting state coherence increases under anesthesia. a) Mean pairwise coherence across electrode sites for awake, isoflurane anesthetized, and ketamine anesthetized animals. Each cell represents the mean coherence between two electrode sites, averaged across pseudo triggers and animals. Cells along the diagonal show the average coherence between signals recorded from the same electrode site, and are thus equal to one. Dotted black regions indicate layer IV. White rectangles border supragranular-infragranular (SG-IG), granular-infragranular (G-IG), and granular-supragranular (G-SG) regions. b) Laminar SG-IG, G-IG, and G-SG coherence against frequency. Interlaminar coherence for each animal was calculated as the average coherence in each region. Bold lines indicate the mean coherence across animals, and dim lines indicate standard error. Shaded regions encompass alpha, beta, and gamma frequency bands and are used in the calculations for (c). c) Mean coherence between 7-90 Hz, averaged across animals. Error bars denote standard error. (n=6 mice: * $p<0.05$)

524 Figure 4: Quantification of evoked multiunit activity. a) Representative peri-stimulus time histograms of
525 evoked responses, recorded from layer V. Each row shows examples from the same mouse at the same
526 electrode site across anesthetics. Evoked responses exhibit dynamic temporal variability across
527 anesthetics. b) Example diagram for how multiunit yield was calculated. MUA was quantified by
528 comparing spike counts, X_S, within a bin of duration, B, at some latency, L, after each stimulus. This
529 distribution of spike counts was then compared to the spike counts within the same bin duration, at
530 some latency, L', before stimulus presentation, using a paired t-test. Analysis was repeated for varying
531 bin sizes and latencies to capture dynamic changes in the evoked response, and then performed on all
532 channels and all animals. c-e) Pseudo-color plots demonstrate the resultant MU yield and signal to
533 noise firing rate ratio (SNFRR, insets). For ease of visualization, all plots show negative latency (L') equal
534 to 0, such that all bin sizes and post-stimulus latencies are compared with the same duration
535 immediately before the stimulus. Awake animals have a consistent, strong transient response, followed
536 by ~100ms of slightly elevated MUA. Alternatively, isoflurane anesthetized animals do not produce a
537 strong transient response, and firing rates are only slightly elevated compared to pre-stimulus intervals.
538 Ketamine anesthesia produces a strong transient response, but periodic bursts of MUA are still observed
539 in the pre-stimulus interval (Fig a, e). Note that the negative SNFRR indicates that firing rates during the
540 pre-stimulus interval exceeded those in the post-stimulus interval, for the parameters specified by B and
541 L. f-g) Parameter values that optimized multiunit yield are shown without the negative latency
542 parameter, as in c-e (f), and with the negative latency parameter (g).
543
544 Figure 5: Laminar responses to visual stimulus further demonstrate temporal variability. a) Multiunit
545 firing rate across depth and time, averaged across 64 stimuli, and then across animals. Stimulus
546 presentation is shown by gray bar. Strong transient responses are observed in awake and ketamine
547 anesthetized mice. Isoflurane reduces the temporal synchrony and prolongs the evoked response.

548 Bursting MUA observed in the spontaneous condition under ketamine anesthesia are apparent in the
549 visually evoked response. b) Induced current source densities, averaged across 64 stimuli, and then
550 across animals. Awake animals demonstrate succinct laminar processing, compared to ketamine.
551 Isoflurane CSD is the weakest and shortest. c-f) Quantification of LFP shows synchronous population
552 activity in the awake case (c-d), and synchronous and sustained population activity under ketamine (c-f).
553 Isoflurane exhibits a weak evoked response. (n=96 electrode sites: * $p<0.001$, % $p=0.02$)
554
555 Figure 6: Visually evoked laminar coherence increases under anesthesia. a) Normalized pairwise
556 coherence, measured as the difference between coherence during ON periods and spontaneous
557 coherence, for awake, isoflurane anesthetized, and ketamine anesthetized animals. b) Evoked SG-IG, G-
558 IG, and G-SG coherence (mean ± standard error) against frequency. Coherence for each animal was
559 calculated as the average coherence in each region encompassed by the white borders in (a). c) Mean
560 coherence between 7-90 Hz (shaded region in (b)), averaged across animals. Error bars denote standard
561 error. (n=6 mice: # $p<0.05$, * $p<0.01$)
562
563 Figure 7: Anesthetics alter rhythmic properties of the evoked response. a) Representative power spectra
564 recorded from layer V, at the same electrode site in the same mouse. Spontaneous power spectra at the
565 same electrode site are shown as dotted lines. Broadband increases in power are observed under
566 anesthesia. b) Power spectra in (a), normalized by subtracting the spontaneous power spectrum from
567 the evoked. A pronounced, visually evoked gamma peak is observed under isoflurane, at slower
568 frequencies than awake. Largest increases in power after visual stimulation under ketamine occur at
569 delta frequencies and across high frequencies. c-d) Anesthesia significantly increases power across the
570 depth of the cortex. e) Power across the depth of the cortex, averaged across 64 stimuli, and then across
571 animals, normalized to resting state as in (b).

Figure 8: Evoked OFF response has similar structure of laminar coherence as ON response. a) Normalized pairwise coherence changes during OFF periods for awake, isoflurane anesthetized, and ketamine anesthetized animals. b) Coherence (mean ± standard error) between SG-IG, G-IG, and G-SG layers. c) Average coherence from 7-90 Hz, averaged across animals. Error bars indicate standard error. (n=6 mice: * $p<0.05$)

REFERENCES

Alkire MT, Hudetz AG, and Tononi G. Consciousness and anesthesia. *Science* 322: 876-880, 2008.

Anver H, Ward PD, Magony A, and Vreugdenhil M. NMDA receptor hypofunction phase couples independent gamma-oscillations in the rat visual cortex. *Neuropsychopharmacology* 36: 519-528, 2011.

Bai D, Pennefather PS, MacDonald JF, and Orser BA. The general anesthetic propofol slows deactivation and desensitization of GABAA receptors. *Journal of Neuroscience* 19: 10635-10646, 1999.

Barrese JC, Rao N, Paroo K, Triebwasser C, Vargas-Irwin C, Franquemont L, and Donoghue JP. Failure mode analysis of silicon-based intracortical microelectrode arrays in non-human primates. *Journal of neural engineering* 10: 066014, 2013.

Bokil H, Andrews P, Kulkarni JE, Mehta S, and Mitra PP. Chronux: a platform for analyzing neural signals. *Journal of neuroscience methods* 192: 146-151, 2010.

Boveroux P, Vanhaudenhuyse A, Bruno M-A, Noirhomme Q, Lauwick S, Luxen A, Degueldre C, Plenevaux A, Schnakers C, and Phillips C. Breakdown of within-and between-network resting state functional magnetic resonance imaging connectivity during propofol-induced loss of consciousness. *Anesthesiology: The Journal of the American Society of Anesthesiologists* 113: 1038-1053, 2010.

Brainard DH. The Psychophysics Toolbox. *Spat Vis* 10: 433-436, 1997.

Brown EN, Purdon PL, and Van Dort CJ. General anesthesia and altered states of arousal: a systems neuroscience analysis. *Annu Rev Neurosci* 34: 601-628, 2011.

Brunel N, and Wang X-J. What determines the frequency of fast network oscillations with irregular neural discharges? I. Synaptic dynamics and excitation-inhibition balance. *Journal of neurophysiology* 90: 415-430, 2003.

Buzsaki G, Anastassiou CA, and Koch C. The origin of extracellular fields and currents--EEG, ECoG, LFP and spikes. *Nat Rev Neurosci* 13: 407-420, 2012.

Buzsáki G, and Wang X-J. Mechanisms of gamma oscillations. *Annual review of neuroscience* 35: 203-225, 2012.

Caixeta FV, Cornelio AM, Scheffer-Teixeira R, Ribeiro S, and Tort AB. Ketamine alters oscillatory coupling in the hippocampus. *Sci Rep* 3: 2348, 2013.

Cardin JA. Snapshots of the brain in action: local circuit operations through the lens of γ oscillations. *Journal of Neuroscience* 36: 10496-10504, 2016.

Carlen M, Meletis K, Siegle JH, Cardin JA, Futai K, Vierling-Claassen D, Ruhlmann C, Jones SR, Deisseroth K, Sheng M, Moore CI, and Tsai LH. A critical role for NMDA receptors in parvalbumin interneurons for gamma rhythm induction and behavior. *Mol Psychiatry* 17: 537-548, 2012.

Cavazzuti M, Porro CA, Biral GP, Benassi C, and Barbieri GC. Ketamine effects on local cerebral blood flow and metabolism in the rat. *Journal of Cerebral Blood Flow & Metabolism* 7: 806-811, 1987.
Cederholm JM, Froud KE, Wong AC, Ko M, Ryan AF, and Housley GD. Differential actions of isoflurane and ketamine-based anaesthetics on cochlear function in the mouse. *Hearing research* 292: 71-79, 2012.
Chauvette S, Crochet S, Volgushev M, and Timofeev I. Properties of slow oscillation during slow-wave sleep and anesthesia in cats. *Journal of Neuroscience* 31: 14998-15008, 2011.
Chery R, Gurden H, and Martin C. Anesthetic regimes modulate the temporal dynamics of local field potential in the mouse olfactory bulb. *Journal of neurophysiology* 111: 908-917, 2014.
Cimenser A, Purdon PL, Pierce ET, Walsh JL, Salazar-Gomez AF, Harrell PG, Tavares-Stoeckel C, Habeeb K, and Brown EN. Tracking brain states under general anesthesia by using global coherence analysis. *Proceedings of the National Academy of Sciences* 108: 8832-8837, 2011.
Cody PA, Eles JR, Lagenaur CF, Kozai TD, and Cui XT. Unique electrophysiological and impedance signatures between encapsulation types: An analysis of biological Utah array failure and benefit of a biomimetic coating in a rat model. *Biomaterials* 161: 117-128, 2018.
Dildy-Mayfield J, Eger E, and Harris R. Anesthetics produce subunit-selective actions on glutamate receptors. *Journal of Pharmacology and Experimental Therapeutics* 276: 1058-1065, 1996.
Douglas RJ, and Martin KA. Neuronal circuits of the neocortex. *Annu Rev Neurosci* 27: 419-451, 2004.
Duncan G, Dreyer D, McKenna T, and Whitsel B. Dose-and time-dependent effects of ketamine on SI neurons with cutaneous receptive fields. *Journal of neurophysiology* 47: 677-699, 1982.
Ehrlichman R, Gandal M, Maxwell C, Lazarewicz M, Finkel L, Contreras D, Turetsky B, and Siegel S. N-methyl-d-aspartic acid receptor antagonist–induced frequency oscillations in mice recreate pattern of electrophysiological deficits in schizophrenia. *Neuroscience* 158: 705-712, 2009.
Ferron J-F, Kroeger D, Chever O, and Amzica F. Cortical inhibition during burst suppression induced with isoflurane anesthesia. *Journal of Neuroscience* 29: 9850-9860, 2009.
Fiáth R, Kerekes BP, Wittner L, Tóth K, Beregszászi P, Horváth D, and Ulbert I. Laminar analysis of the slow wave activity in the somatosensory cortex of anesthetized rats. *European Journal of Neuroscience* 44: 1935-1951, 2016.
Franks NP. General anaesthesia: from molecular targets to neuronal pathways of sleep and arousal. *Nature reviews Neuroscience* 9: 370, 2008.
Fries P. Neuronal gamma-band synchronization as a fundamental process in cortical computation. *Annual review of neuroscience* 32: 209-224, 2009.
Fries P, Reynolds JH, Rorie AE, and Desimone R. Modulation of oscillatory neuronal synchronization by selective visual attention. *Science* 291: 1560-1563, 2001.
Furmaga H, Park H-J, Cooperrider J, Baker KB, Johnson M, Gale JT, and Machado AG. Effects of ketamine and propofol on motor evoked potentials elicited by intracranial microstimulation during deep brain stimulation. *Frontiers in systems neuroscience* 8: 2014.
Garcia PS, Kolesky SE, and Jenkins A. General anesthetic actions on GABA(A) receptors. *Curr Neuropharmacol* 8: 2-9, 2010.
Goltstein PM, Montijn JS, and Pennartz CM. Effects of isoflurane anesthesia on ensemble patterns of Ca2+ activity in mouse v1: reduced direction selectivity independent of increased correlations in cellular activity. *PLoS One* 10: e0118277, 2015.
Haider B, Hausser M, and Carandini M. Inhibition dominates sensory responses in the awake cortex. *Nature* 493: 97-100, 2013.
Hakami T, Jones NC, Tolmacheva EA, Gaudias J, Chaumont J, Salzberg M, O'Brien TJ, and Pinault D. NMDA receptor hypofunction leads to generalized and persistent aberrant γ oscillations independent of hyperlocomotion and the state of consciousness. *PLoS One* 4: e6755, 2009.
Hasenstaub A, Sachdev RN, and McCormick DA. State changes rapidly modulate cortical neuronal responsiveness. *Journal of Neuroscience* 27: 9607-9622, 2007.

Hayton S, Kriss A, and Muller D. Comparison of the effects of four anaesthetic agents on somatosensory evoked potentials in the rat. *Laboratory animals* 33: 243-251, 1999.
Henze DA, Borhegyi Z, Csicsvari J, Mamiya A, Harris KD, and Buzsaki G. Intracellular features predicted by extracellular recordings in the hippocampus in vivo. *J Neurophysiol* 84: 390-400, 2000.
Hirsch JA, and Martinez LM. Laminar processing in the visual cortical column. *Current opinion in neurobiology* 16: 377-384, 2006.
Homayoun H, and Moghaddam B. NMDA receptor hypofunction produces opposite effects on prefrontal cortex interneurons and pyramidal neurons. *J Neurosci* 27: 11496-11500, 2007.
Hudetz AG. General anesthesia and human brain connectivity. *Brain connectivity* 2: 291-302, 2012.
Imas O, Ropella K, Wood J, and Hudetz A. Halothane augments event-related γ oscillations in rat visual cortex. *Neuroscience* 123: 269-278, 2004.
Imas OA, Ropella KM, Ward BD, Wood JD, and Hudetz AG. Volatile anesthetics enhance flash-induced gamma oscillations in rat visual cortex. *Anesthesiology* 102: 937-947, 2005.
Jia X, Smith MA, and Kohn A. Stimulus selectivity and spatial coherence of gamma components of the local field potential. *Journal of Neuroscience* 31: 9390-9403, 2011.
Kaneko T, Yokoyama K, and Makita K. Late preconditioning with isoflurane in cultured rat cortical neurones. *British journal of anaesthesia* 95: 662-668, 2005.
Kimbro JR, Kelly PJ, Drummond JC, Cole DJ, and Patel PM. Isoflurane and pentobarbital reduce AMPA toxicity in vivo in the rat cerebral cortex. *The Journal of the American Society of Anesthesiologists* 92: 806-812, 2000.
Kleiner M, Brainard D, Pelli D, Ingling A, Murray R, and Broussard C. What's new in Psychtoolbox-3. *Perception* 36: 1, 2007.
Klimesch W, Sauseng P, and Hanslmayr S. EEG alpha oscillations: the inhibition–timing hypothesis. *Brain research reviews* 53: 63-88, 2007.
Kolarcik CL, Luebben SD, Sapp SA, Hanner J, Snyder N, Kozai TDY, Chang E, Nabity JA, Nabity ST, Lagenaur CF, and Cui XT. Elastomeric and soft conducting microwires for implantable neural interfaces. *Soft Matter* 11: 4847-4861, 2015.
Kolta A, Diop L, and Reader TA. Noradrenergic effects on rat visual cortex: Single-cell microiontophoretic studies of alpha-2 adrenergic receptors. *Life sciences* 41: 281-289, 1987.
Kozai TD, Catt K, Du Z, Na K, Srivannavit O, Razi-ul MH, Seymour J, Wise KD, Yoon E, and Cui XT. Chronic in vivo evaluation of PEDOT/CNT for stable neural recordings. *IEEE Transactions on Biomedical Engineering* 63: 111-119, 2016.
Kozai TD, Catt K, Li X, Gugel ZV, Olafsson VT, Vazquez AL, and Cui XT. Mechanical failure modes of chronically implanted planar silicon-based neural probes for laminar recording. *Biomaterials* 37: 25-39, 2015a.
Kozai TD, Du Z, Gugel ZV, Smith MA, Chase SM, Bodily LM, Caparosa EM, Friedlander RM, and Cui XT. Comprehensive chronic laminar single-unit, multi-unit, and local field potential recording performance with planar single shank electrode arrays. *Journal of neuroscience methods* 242: 15-40, 2015b.
Kozai TD, Langhals NB, Patel PR, Deng X, Zhang H, Smith KL, Lahann J, Kotov NA, and Kipke DR. Ultrasmall implantable composite microelectrodes with bioactive surfaces for chronic neural interfaces. *Nat Mater* 11: 1065-1073, 2012.
Kozai TD, Li X, Bodily LM, Caparosa EM, Zenonos GA, Carlisle DL, Friedlander RM, and Cui XT. Effects of caspase-1 knockout on chronic neural recording quality and longevity: insight into cellular and molecular mechanisms of the reactive tissue response. *Biomaterials* 35: 9620-9634, 2014.
Kremkow J, Jin J, Komban SJ, Wang Y, Lashgari R, Li X, Jansen M, Zaidi Q, and Alonso J-M. Neuronal nonlinearity explains greater visual spatial resolution for darks than lights. *Proceedings of the National Academy of Sciences* 111: 3170-3175, 2014.

Lehmann K, Schmidt K-F, and Löwel S. Vision and visual plasticity in ageing mice. *Restorative neurology and neuroscience* 30: 161-178, 2012.
Ludwig KA, Miriani RM, Langhals NB, Joseph MD, Anderson DJ, and Kipke DR. Using a common average reference to improve cortical neuron recordings from microelectrode arrays. *Journal of neurophysiology* 101: 1679-1689, 2009.
Maier A, Adams GK, Aura C, and Leopold DA. Distinct superficial and deep laminar domains of activity in the visual cortex during rest and stimulation. *Frontiers in systems neuroscience* 4: 31, 2010.
Mashour GA, and Hudetz AG. Neural Correlates of Unconsciousness in Large-Scale Brain Networks. *Trends in neurosciences* 2018.
Mechler F, and Victor JD. Dipole characterization of single neurons from their extracellular action potentials. *Journal of Computational Neuroscience* 32: 73-100, 2012.
Mendelson J, and Wells E. Age-related changes in the visual cortex. *Vision Research* 42: 695-703, 2002.
Michelson NJ, Vazquez AL, Eles JR, Salatino JW, Purcell EK, Williams JJ, Cui T, and Kozai TDY. Multi-scale, multi-modal analysis uncovers complex relationship at the brain tissue-implant neural interface: New Emphasis on the Biological Interface. *Journal of neural engineering* 2017.
Mitra P. *Observed brain dynamics*. Oxford University Press, 2007.
Pelli DG. The VideoToolbox software for visual psychophysics: transforming numbers into movies. *Spat Vis* 10: 437-442, 1997.
Petermann T, Thiagarajan TC, Lebedev MA, Nicolelis MA, Chialvo DR, and Plenz D. Spontaneous cortical activity in awake monkeys composed of neuronal avalanches. *Proceedings of the National Academy of Sciences* 106: 15921-15926, 2009.
Polidori C, Zeng Y-C, Zaccheo D, and Amenta F. Age-related changes in the visual cortex: a review. *Archives of gerontology and geriatrics* 17: 145-164, 1993.
Ray S, and Maunsell JH. Differences in gamma frequencies across visual cortex restrict their possible use in computation. *Neuron* 67: 885-896, 2010.
Ray S, and Maunsell JH. Do gamma oscillations play a role in cerebral cortex? *Trends Cogn Sci* 19: 78-85, 2015.
Robinson DH, and Toledo AH. Historical development of modern anesthesia. *Journal of Investigative Surgery* 25: 141-149, 2012.
Ruebhausen M, Brozoski T, and Bauer C. A comparison of the effects of isoflurane and ketamine anesthesia on auditory brainstem response (ABR) thresholds in rats. *Hearing research* 287: 25-29, 2012.
Sarasso S, Boly M, Napolitani M, Gosseries O, Charland-Verville V, Casarotto S, Rosanova M, Casali AG, Brichant J-F, and Boveroux P. Consciousness and complexity during unresponsiveness induced by propofol, xenon, and ketamine. *Current Biology* 25: 3099-3105, 2015.
Schroeder KE, Irwin ZT, Gaidica M, Bentley JN, Patil PG, Mashour GA, and Chestek CA. Disruption of corticocortical information transfer during ketamine anesthesia in the primate brain. *Neuroimage* 134: 459-465, 2016.
Self MW, Kooijmans RN, Supèr H, Lamme VA, and Roelfsema PR. Different glutamate receptors convey feedforward and recurrent processing in macaque V1. *Proceedings of the National Academy of Sciences* 109: 11031-11036, 2012.
Sellers KK, Bennett DV, Hutt A, and Frohlich F. Anesthesia differentially modulates spontaneous network dynamics by cortical area and layer. *J Neurophysiol* 110: 2739-2751, 2013.
Sellers KK, Bennett DV, Hutt A, Williams JH, and Frohlich F. Awake vs. anesthetized: layer-specific sensory processing in visual cortex and functional connectivity between cortical areas. *J Neurophysiol* 113: 3798-3815, 2015.
Shaw AD, Saxena N, L EJ, Hall JE, Singh KD, and Muthukumaraswamy SD. Ketamine amplifies induced gamma frequency oscillations in the human cerebral cortex. *Eur Neuropsychopharmacol* 25: 1136-1146, 2015.

Shu Y, Hasenstaub A, and McCormick DA. Turning on and off recurrent balanced cortical activity. *Nature* 423: 288, 2003.
Sigel E, and Steinmann ME. Structure, function, and modulation of GABA(A) receptors. *J Biol Chem* 287: 40224-40231, 2012.
Singer W, and Gray CM. Visual feature integration and the temporal correlation hypothesis. *Annual review of neuroscience* 18: 555-586, 1995.
Smith GB, Whitney DE, and Fitzpatrick D. Modular representation of luminance polarity in the superficial layers of primary visual cortex. *Neuron* 88: 805-818, 2015.
Steriade M, Contreras D, Dossi RC, and Nunez A. The slow (< 1 Hz) oscillation in reticular thalamic and thalamocortical neurons: scenario of sleep rhythm generation in interacting thalamic and neocortical networks. *Journal of Neuroscience* 13: 3284-3299, 1993a.
Steriade M, Nunez A, and Amzica F. A novel slow (< 1 Hz) oscillation of neocortical neurons in vivo: depolarizing and hyperpolarizing components. *Journal of neuroscience* 13: 3252-3265, 1993b.
Supp GG, Siegel M, Hipp JF, and Engel AK. Cortical hypersynchrony predicts breakdown of sensory processing during loss of consciousness. *Current biology* 21: 1988-1993, 2011.
Tononi G. Consciousness as integrated information: a provisional manifesto. *The Biological Bulletin* 215: 216-242, 2008.
van Kerkoerle T, Self MW, Dagnino B, Gariel-Mathis MA, Poort J, van der Togt C, and Roelfsema PR. Alpha and gamma oscillations characterize feedback and feedforward processing in monkey visual cortex. *Proc Natl Acad Sci U S A* 111: 14332-14341, 2014.
Wang X-J, and Buzsáki G. Gamma oscillation by synaptic inhibition in a hippocampal interneuronal network model. *Journal of neuroscience* 16: 6402-6413, 1996.
Wellman SM, Eles JR, Ludwig KA, Seymour JP, Michelson NJ, McFadden WE, Vazquez AL, and Kozai TD. A materials roadmap to functional neural interface design. *Advanced Functional Materials* 2017.
Woodward WR, Choi D, Grose J, Malmin B, Hurst S, Pang J, Weleber RG, and Pillers D-AM. Isoflurane is an effective alternative to ketamine/xylazine/acepromazine as an anesthetic agent for the mouse electroretinogram. *Documenta Ophthalmologica* 115: 187-201, 2007.
Worden MS, Foxe JJ, Wang N, and Simpson GV. Anticipatory biasing of visuospatial attention indexed by retinotopically specific-band electroencephalography increases over occipital cortex. *J Neurosci* 20: 1-6, 2000.

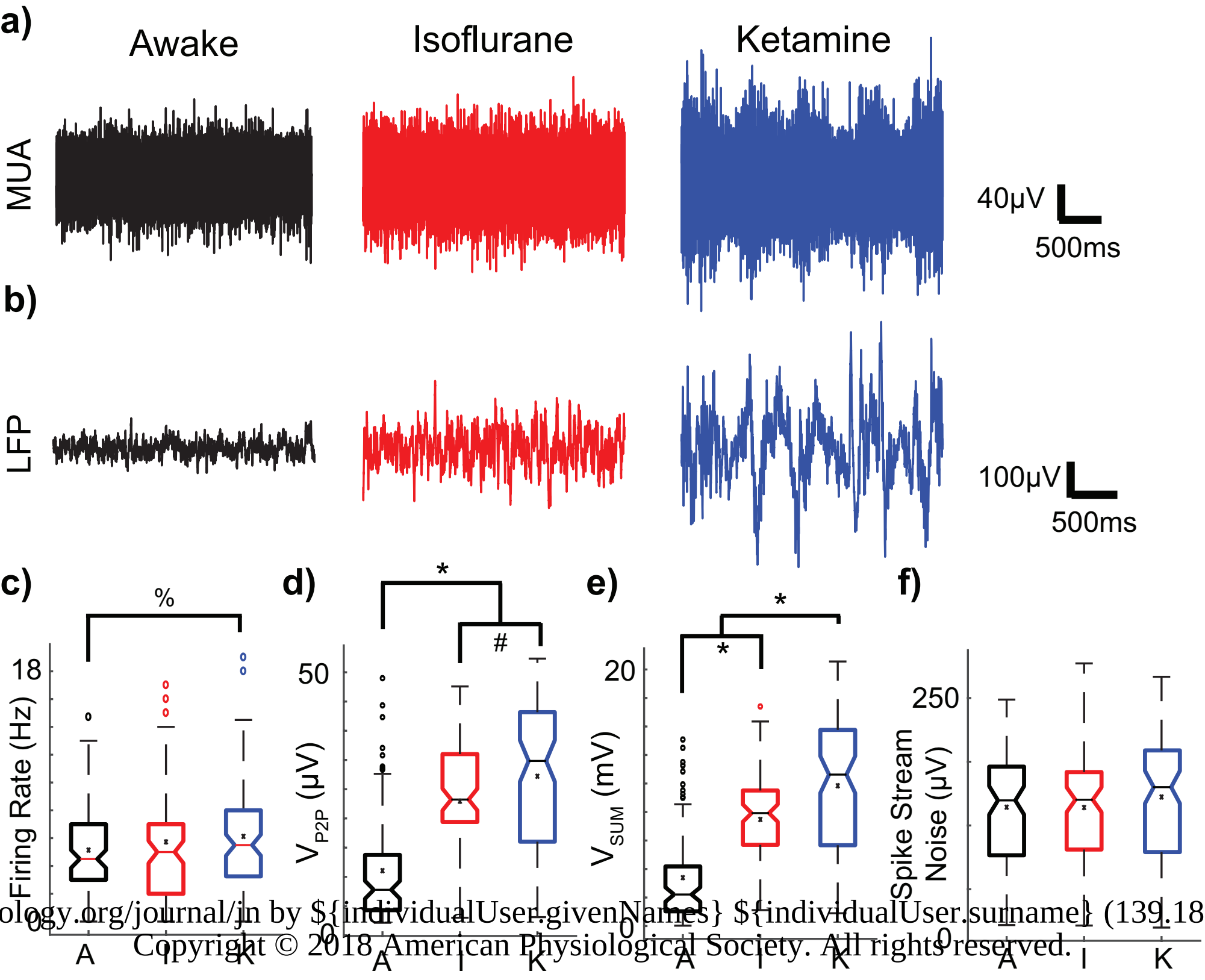

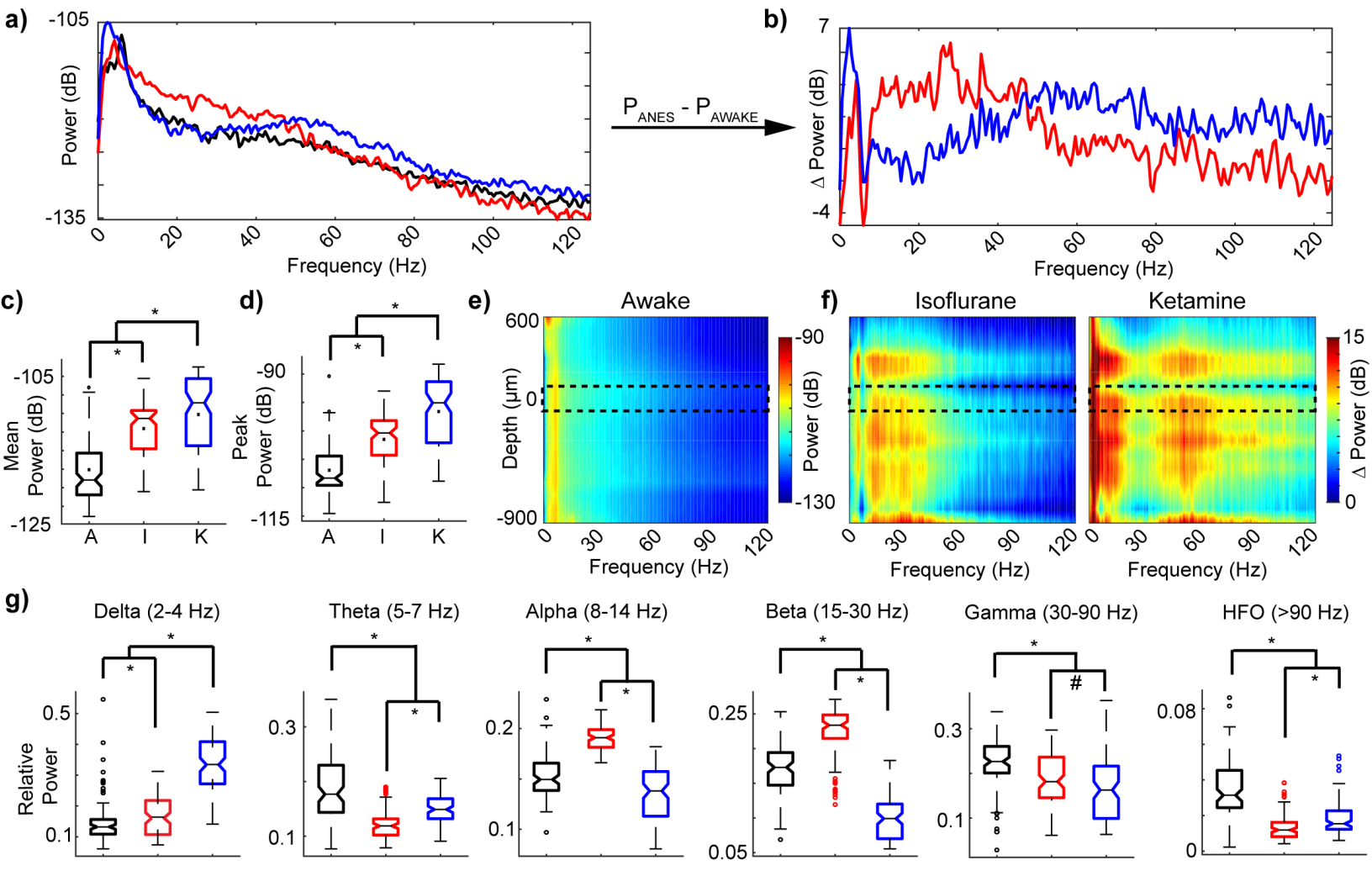

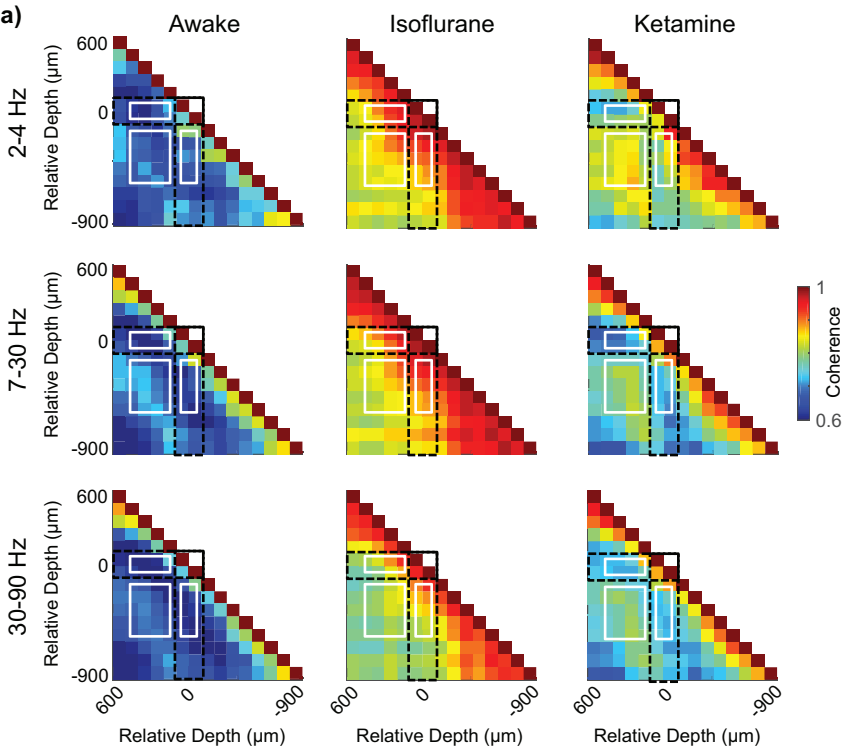

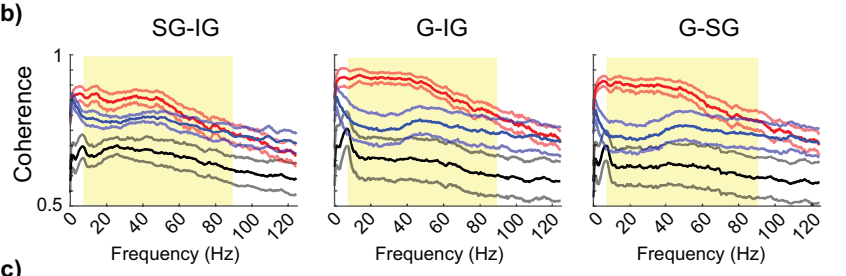

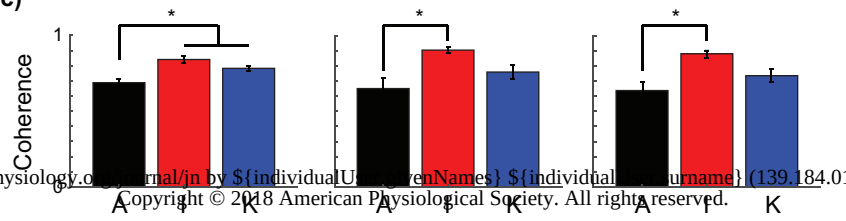

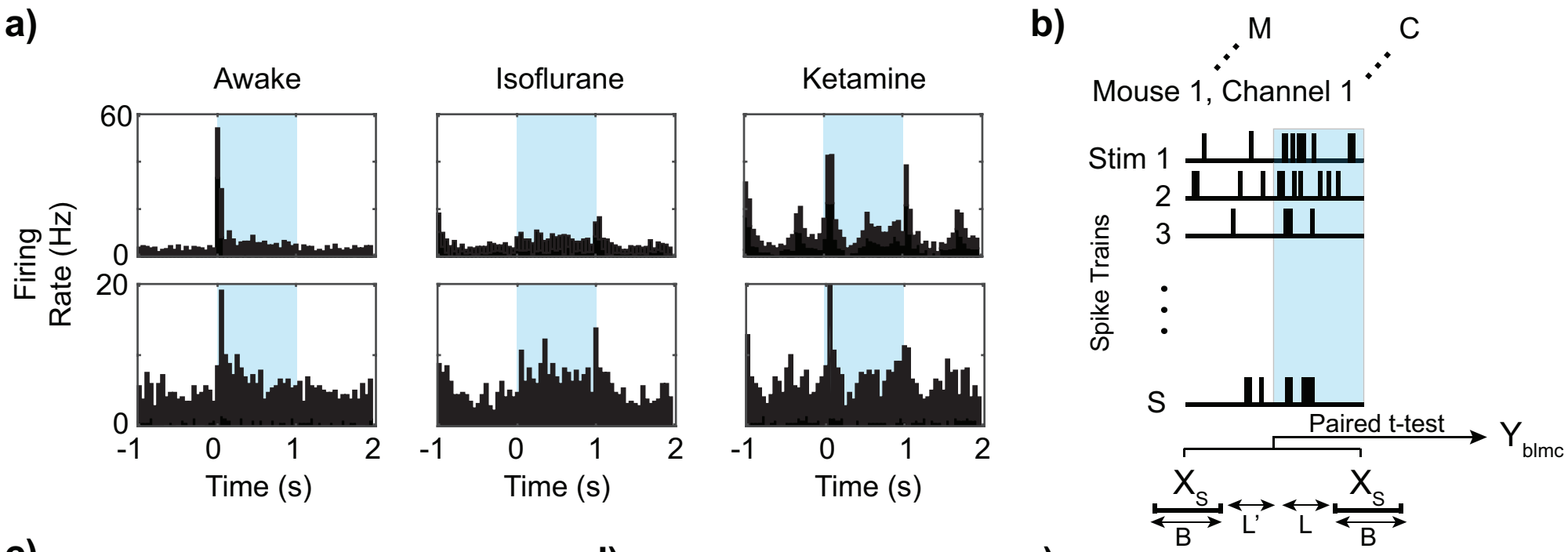

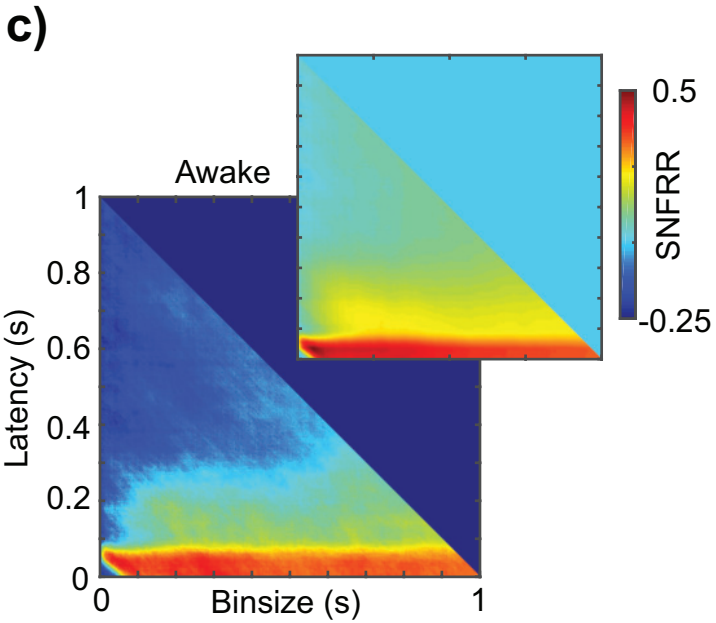

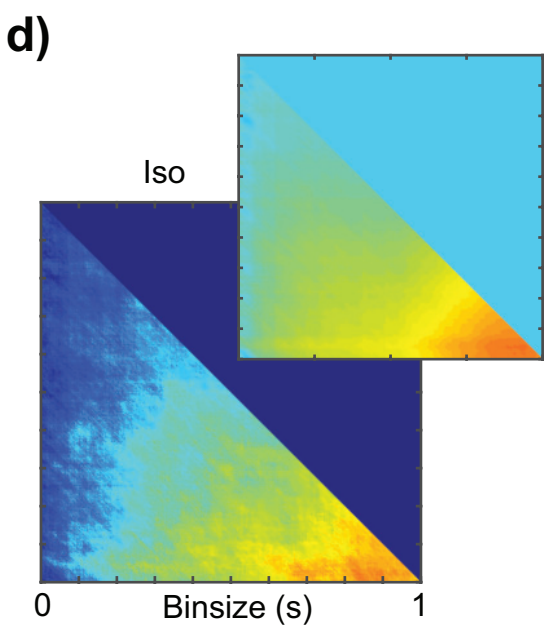

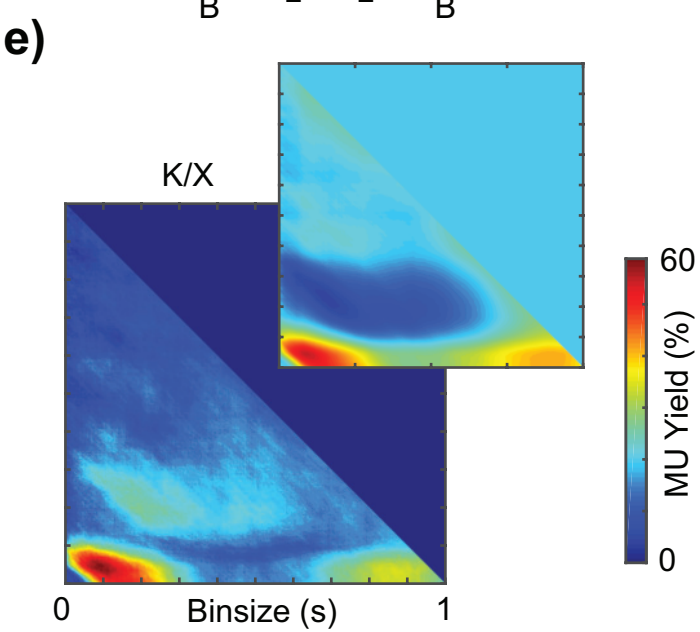

f)

	B (ms)	L (ms)	L' (ms)	Yield (%)	SNFRR
Awake	66.5	30.5	0	54.0	0.49
Iso	840.5	18.0	0	45.8	0.31
K/X	101.5	49.0	58.5	58.0	0.44

g)

	B (ms)	L (ms)	L' (ms)	Yield (%)	SNFRR
Awake	59	39	15	56.3	0.47
Iso	835	21	59	50	0.31
K/X	94	38	17	60.2	0.44